IEICE TRANS. COMMUN., VOL.E105–B, NO.1 JANUARY 2022

PAPER

Study in CSI Correction Localization Algorithm with DenseNet

Junna SHANG[†a)], ***Nonmember and*** **Ziyang YAO**[†b)], ***Student Member***

SUMMARY With the arrival of 5G and the popularity of smart devices, indoor localization technical feasibility has been verified, and its market demands is huge. The channel state information (CSI) extracted from Wi-Fi is physical layer information which is more fine-grained than the received signal strength indication (RSSI). This paper proposes a CSI correction localization algorithm using DenseNet, which is termed CorFi. This method first uses isolation forest to eliminate abnormal CSI, and then constructs a CSI amplitude fingerprint containing time, frequency and antenna pair information. In an offline stage, the densely connected convolutional networks (DenseNet) are trained to establish correspondence between CSI and spatial position, and generalized extended interpolation is applied to construct the interpolated fingerprint database. In an online stage, DenseNet is used for position estimation, and the interpolated fingerprint database and K-nearest neighbor (KNN) are combined to correct the position of the prediction results with low maximum probability. In an indoor corridor environment, the average localization error is 0.536 m.

key words: *channel state information, indoor localization, fingerprinting, deep neural network, generalized extended interpolation, isolation forest*

1. Introduction

There are many requirements of location-based services in indoor environments, e.g., intelligent business district, hospital, nursing home, intelligent logistic warehouse, skyscraper, underground parking, etc. Because the signal is blocked or corrupted by dense obstructions, Global Navigation Satellite System (GNSS) can't provide high accuracy navigation and localization inside the building. Therefore, various indoor positioning technologies are developed, such as pedestrian dead reckoning, ultra wide bandwidth, visible light, magnetic fields, Bluetooth and ultrasound [1]–[6]. Many recent studies use RSSI or CSI extracted from Wi-Fi has been applied widely to estimate position.

PinLoc [7], [8] is the first Wi-Fi localization system based on physical layer information that uses a commercial network interface cards (NICs). FILA [9] is a system using CSI for triangulation method. It trains the indoor propagation model for each indoor environment, and the location estimation use triangulation method according to the model and the line-of-sight (LOS) or the shortest Non-Line-of-Sight (NLOS) received CSI. The Fine-grained Indoor Fingerprinting System (FIFS) [10] divides 20 MHz bandwidth into four subchannels equally and uses the sum of each subchannel power as fingerprint. CSI-MIMO [11] proposes a fingerprint combined with amplitude and phase of CSI, which uses the frequency diversity of CSI appropriately. DeepFi [12] is a deep-learning-based indoor fingerprinting system using Bayesian estimator, which uses CSI amplitude as fingerprint, while the calibrated CSI phase are used in PhaseFi [13]. Some works optimize a centroid algorithm based on CSI propagation model, and they estimate location by KNN [14]. Considering the channel at a fixed location is stable, Wu et al. [15] propose Time Reversal Resonating Strength (TRRS) based on Time Reversal (TR) radio transmission, and they use TRRS based on Channel Impulse Response (CIR) for inverse Fourier transform of CSI to measure the similarity of test data and training data. Moreover, RSSI and CSI are both applied in some systems to fully utilize transmission channel quality metrics [16], [17].

Indoor localization system based on CSI with high research value has high accuracy without expensive equipment. The key of further improving the accuracy and robustness of this localization system is sufficient extraction and reasonable application of CSI data features. Based on existing CSI-based indoor localization algorithms, we use DenseNet to establish correspondence between CSI and spatial position, and interpolated fingerprint database and K-nearest neighbor algorithm are applied to correct the position of the prediction results when the reliability of probability weighted localization algorithm based on neural network is low. The experiment results show that this method reduces the localization error of probability weighted localization algorithm based on neural network, and compensates the shortcomings of a single algorithm effectively to improve the stability of indoor localization.

2. CSI Data Characteristics

IEEE 802.11a uses orthogonal frequency division multiplexing (OFDM) technology to exploit 52 OFDM subcarriers that can be read through some NICs, such as Intel's IWL 5300, Atheros [18]. Take IWL 5300 NICs as an example, we can acquire 30 subcarriers by this NIC, and each subcarrier can be written as Eq. (1).

$$H(k) = |H(k)| \cdot e^{j\angle H(k)} \tag{1}$$

where $|H(k)|$ and $\angle H(k)$ are the amplitude and phase of subcarrier k respectively. The CSI data is a three dimensional

Manuscript received March 6, 2021.
Manuscript revised May 8, 2021.
Manuscript publicized June 23, 2021.

[†]The authors are with College of Telcommunication Engineering, Hangzhou Dianzi University, Hangzhou 310018, China.
a) E-mail: shangjn@hdu.edu.cn
b) E-mail: yaoziyang@hdu.edu.cn

DOI: 10.1587/transcom.2021EBP3033

matrix, which represents transmitting antenna, receiving antenna and subcarrier respectively. The receiving antennas are expressed in descending order of RSS. Every elements of matrix is the real and imaginary parts of a subcarrier that can be converted to amplitude and phase. As mentioned previously, CIR can be obtained by inverse Fourier transform of CSI, which is able to distinguish multipath signals. The time resolution is 50 ns when the bandwidth is 20 MHz, so CIR can distinguish smaller scale multipath with higher bandwidth.

Whether a data can be used for fingerprinting needs to satisfy two conditions that the data features of the same category show strong stability and the data features of different categories show dissimilarity. The paper [7], [19] propose that CSI amplitude values exhibit great stability at a fixed location compared with RSS values, which is validated by abundant experiments. The main reason of different locations have different CSI is multipath effect.

Considering two propagation paths with the same attenuation, the expressions at the receiver are $Af(t-\tau_1)$ and $Af(t-\tau_2)$ respectively, where τ_1 and τ_2 are the time taken for signals of two propagation paths to the receiver, A is the attenuation coefficient. We set the Fourier transform of signal $f(t)$ to $F(\omega)$, then the spectrum function of the received signal is shown in Eq. (2).

$$AF(\omega)e^{-j\omega\tau_1}\left(1+e^{-j\omega(\tau_2-\tau_1)}\right) \tag{2}$$

and the transfer function of multipath channel is

$$Ae^{-j\omega\tau_1}\left(1+e^{-j\omega(\tau_2-\tau_1)}\right) \tag{3}$$

where $e^{-j\omega\tau_1}$ is a certain transmission delay, and the modulus of the items in brackets is

$$\left|1+e^{-j\omega(\tau_2-\tau_1)}\right| = 2\left|\cos\frac{\omega(\tau_2-\tau_1)}{2}\right| \tag{4}$$

It can be seen that the propagation attenuation of multipath is related to signal frequency and delay difference. In practice, a multipath channel has more than two propagation paths, and the attenuation of each path is different, but the envelope of the received signal must fluctuate randomly.

Figure 1 shows feature images from two adjacent reference points (RP) at three different times. It can be seen that the features of the same RP show strong stability at different times and the features of different RPs show obvious dissimilarity. There are 32 rows and 30 columns in fingerprint, and each column corresponds to the 30 subcarriers. Rows 1 to 8 are samples of the first pair of antennas from 8 continuously received packets, rows 9 to 16 are packets of the second pair of antennas from same packets, and so on. We created 4 antenna Pairs and each of them has CSI of two antennas of transmission and reception. It can be seen from Fig. 1 that the CSI of same antenna pair are similar, while the CSI of different antenna pairs are different and it improves the stability of matching fingerprints.

In the experiment, it was found that CSI data at a fixed location has multiple clusters in some cases which brings a problem of removing abnormal samples. The main reason of this phenomenon is multipath effect [12]. Conventional anomaly detection methods such as three-sigma rule, box plot are based on the normal distribution. Taking Fig. 2(a) as an example, these methods won't be able to eliminate the abnormal samples indicated by the red arrows. There are many reasons for these irregular and non-repeatable abnormal samples, such as interference from other sources, or random people walking, etc. Therefore, we remove the abnormal samples that may be harmful to fingerprinting.

We use Isolation Forest (iForest) [20], [21] to eliminate abnormal CSI samples. Isolation Forest is an ingenious method for detecting anomalies without statistical parameters such as mean and variance. Figure 3 shows that the distribution of a set of data in a certain dimension *Dim*.

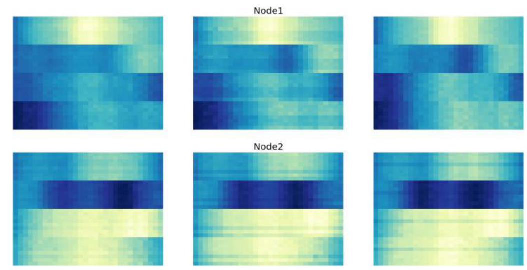

Fig. 1 Feature images from two RPs at different times.

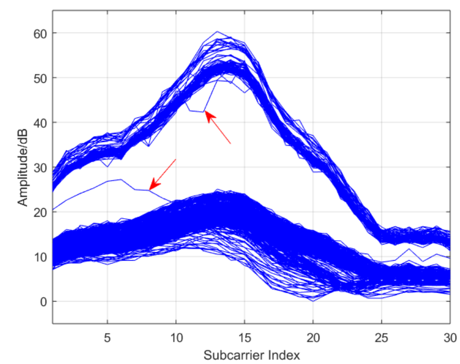

(a) Original data

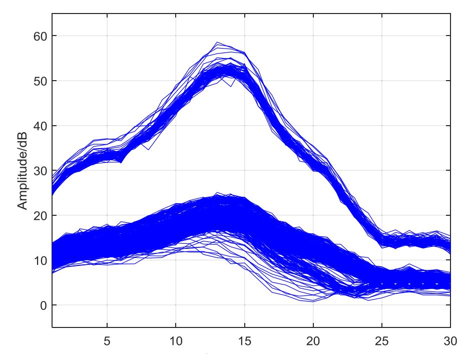

(b) Data processed by Isolation Forest

Fig. 2 Amplitude of continuously received CSI at a fixed location.

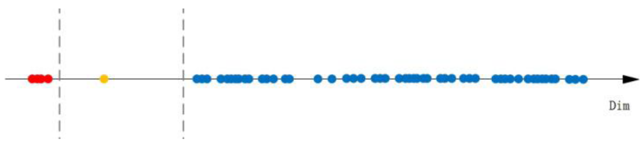

Fig. 3 Isolation Forest example.

If we chose a random number between the maximum and minimum values of all samples in this dimension, we can separate the data set to two parts that are greater than this number and less than or equal to this number. It is more likely that normal data, such as the blue dots in the Fig. 3, will need more cuts to be separated than abnormal data such as the yellow dots.

Isolation Forest is based on this premise, and random selecting dimensions with abundant isolated trees and randomly cuts are used to avoid contingency. The anomaly score [20] is used to determine if the sample is abnormal, and the anomaly score of sample s in a data set is

$$score(s) = 2^{-\frac{E(cut(s))}{APL(S)}}$$
$$APL(S) = 2 \cdot (\ln(S-1) + \gamma) - \frac{2 \cdot (S-1)}{S} \tag{5}$$

Where $E(\cdot)$ means calculating the mean value, $cut(s)$ is the number of times and sample s is cut in an isolated tree, S is the number of the samples, and $APL(S)$ is the average path length for the data set. The higher the anomaly score, the more likely the sample is abnormal. As shown in Fig. 2(b), abnormal CSI have been eliminated by iForest.

3. System Development

In this paper, we study how to use deep neural network to utilize CSI for indoor localization, and how to improve the accuracy of localization with KNN. The main idea of the localization algorithm is fingerprint positioning divided into offline stage and online stage, and the localization algorithm architecture is shown in Fig. 4.

3.1 Data Collection

We use one transmitter with two antennas in this paper. In offline stage, the data of all RPs are collected at first. For the i-th RP, n CSI packets are collected: $CSI_i = \left(csi_i^1, csi_i^2, \ldots, csi_i^j, \ldots, csi_i^n\right)$, and each packet is

$$csi_i^j = \begin{bmatrix} H_{11}^{ij} & H_{12}^{ij} & \cdots & H_{1k}^{ij} & \cdots & H_{1K}^{ij} \\ H_{21}^{ij} & H_{22}^{ij} & \cdots & H_{2k}^{ij} & \cdots & H_{2K}^{ij} \\ \vdots & \vdots & \ddots & \vdots & & \vdots \\ H_{p1}^{ij} & H_{p2}^{ij} & \cdots & H_{pk}^{ij} & \cdots & H_{pK}^{ij} \\ \vdots & \vdots & & \vdots & \ddots & \vdots \\ H_{P1}^{ij} & H_{P2}^{ij} & \cdots & H_{Pk}^{ij} & \cdots & H_{PK}^{ij} \end{bmatrix} \tag{6}$$

where i is the number of RPs, which is the category. H_{pk}^{ij} is the CSI of the k-th subcarrier of the p-th antenna pair of the j-th packet of the i-th RP. The CSI training data set with N RPs is $CSI_{train} = \{(CSI_i, l_i)\}_{i=1}^{N}$, $l_i = (x_i, y_i)$, where l_i is the coordinate of the i-th RP.

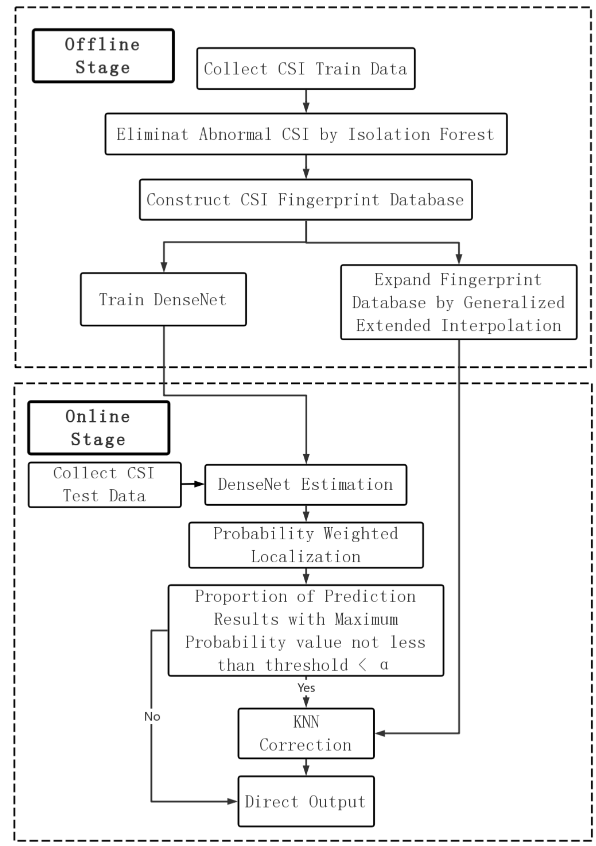

Fig. 4 CSI correction localization algorithm with DenseNet architecture.

Take all samples of the k-th subcarrier of the p-th antenna pair on the i-th RP as a unit and use iForest to obtain the abnormal data packet number. After each subcarrier and each antenna pair has undergone anomaly detection, we merge these abnormal numbers and remove duplicates to get the abnormal number set of the i-th RP. The abnormal samples are eliminated according to this set, and the number of samples retained is n_i. Finally, we have CSI'_{train} that has been eliminated abnormal samples.

3.2 Interpolation and Fingerprint Database

In fingerprinting scheme, an appropriate interpolation can not only reduce manpower cost in offline stage, but also improve localization performance. Generalized extended interpolation is a segmentation approximation method that combines interpolation and fitting methods satisfies the interpolation conditions at the segment boundary to ensure good continuity between the segments, also combine the internal and external segments RPs to achieve the best fit in the segment [22]. In the experiment and simulation verification interpolation fingerprint, generalized extended interpolation is more accurate than the conventional interpolation method

[23].

Before interpolation, each RP is averaged, and the mean vector of the i-th RP is $\overline{csi_i} = \left[\left|\overline{H}_1^i\right| \left|\overline{H}_2^i\right| \ \dots \ \left|\overline{H}_k^i\right| \ \dots \ \left|\overline{H}_K^i\right|\right]$, and any element is the average of all samples:

$$\left|\overline{H}_k^i\right| = \frac{1}{n_i}\frac{1}{P}\sum_{j=1}^{n_i}\sum_{p=1}^{P}\left|H_{pk}^{ij}\right| \tag{7}$$

For each element, a generalized extended interpolation is used in the entire fingerprint database. The number of new RPs depends on the step size and the distribution of the original RPs. After adding the original RPs, there are M RPs in total, and the fingerprint is $\overline{csi_m} = \left(\left|\overline{H}_1^m\right|, \left|\overline{H}_2^m\right|, \dots, \left|\overline{H}_k^m\right|, \dots, \left|\overline{H}_K^m\right|\right)$. The interpolated fingerprint database after generalized extended interpolation is $CSI_{insert} = \left\{\left(\overline{csi_m}, l_m\right)\right\}_{m=1}^{M}$, $l_m = (x_m, y_m)$. The mean CSI test database is $CSI_{test} = \left\{\left(\overline{csi_q}, l_q\right)\right\}_{q=1}^{Q}$, $l_q = \left(x_q, y_q\right)$ correspondingly, where $\overline{csi_q}$ is fingerprint of q-th test node and Q is the number of test nodes.

We use data from CSI'_{train} as training data to construct feature images. For n_i samples of each RP, we use sliding window to group in order. The size of the sliding window is W, that is, W continuous samples are used to construct one fingerprint until the rest of samples out of n_i samples are less than W. There are $n_i \backslash W$ ($\backslash$ is Integer Division) fingerprints for the i-th RP. In the experiment, W is 8, and the CSI amplitudes of the first pair of antenna pairs of 8 samples are arranged in rows until the last pair of antenna pairs is arranged. As shown in Fig. 1, one feature image has 32 rows and 30 columns, and some features such as vertical lines are easy to be captured by multiple samples instead of a single-shot. Thus, we have the training fingerprint database: $FingerCSI_{Train} = \left\{\left(CSI_{WP\times K,i}, l_i\right)\right\}_{i=1}^{N_F^{Train}}$, where N_F^{Train} is the number of fingerprints.

The construction method of the test fingerprint database in online stage is similar to the training fingerprint database in offline stage. However, we use box plot instead of iForest to eliminate abnormal samples, because the distribution of test data is consistent in a short period of time. The test fingerprint database is $FingerCSI_{Test} = \left\{\left(CSI_{WP\times K,i}, l_i\right)\right\}_{i=1}^{N_F^{Test}}$.

3.3 CSI Localization DenseNet

DenseNet [24] is a convolutional neural network that stacks the output of the previous layer of the network and the input of the current layer on the channel dimension to alleviate the vanishing gradient problem. On the one hand, the dense connection not only alleviates the vanishing gradient and model degradation problems, but also enhances the reuse of features, which facilitates the transfer of information between layers, and also provides more possibilities for model construction. On the other hand, the number of parameters of DenseNet is significantly less than the Residual Network (ResNets) that is also used to alleviate the vanishing gradient problem. Moreover, it's less than conventional convolutional neural network, and DenseNet has high parameter efficient. DenseNet has two main components, one is dense block, the other is transition layer. The main body of DenseNet is alternately stacked by dense blocks and transition layers, and the head and tail are both dense blocks.

The unique structure of DenseNet is very conducive to building the model of CSI and spatial position. In this paper, we modify the original DenseNet to adapt to CSI fingerprint location classification. First of all, CSI data at a fixed location sometimes has multiple clusters, and it contains noise generally. In the original network, the activation function is Rectified Linear Unit (ReLU), which is fragile during training. When a large gradient flows through a ReLU to update weights, it may no longer be activated by other data, which is not conducive to the network to learn the correspondence between CSI fingerprint and location. We substitute Exponential Linear Unit (ELU) [25] for the original activation function ReLU. When the input is negative, the derivative of ELU is not equal to zero, which can alleviate the problem of 'dead neuron'. The activation function formula is

$$f(x)=\begin{cases} x & x>0 \\ \alpha(\exp(x)-1) & x\le 0 \end{cases}, \quad f'(x)=\begin{cases} 1 & x>0 \\ f(x)+\alpha & x\le 0 \end{cases} \tag{8}$$

where α is the ELU hyperparameter. Another advantage of ELU is that its derivative goes to zero when the input goes to negative infinity, which is conducive to deal with noise of CSI.

Secondly, we use multiple fully-connected layers at the end of the network. The features extracted by the convolutional layer at the front of the network are integrated through the fully-connected layer, and then the data is non-linearly transformed to complete the classification. The input data is CSI feature images from $FingerCSI_{train}$, and the output label is a one-hot position classification vector with dimension N: $Label = (L_1, L_2, \dots, L_i, \dots, L_N)$. The output layer is calculated by softmax function:

$$p_i = \frac{e^{h_{ii}}}{\sum_{ii=1}^{N} e^{h_{ii}}} \tag{9}$$

where $(h_1, h_2, \dots, h_i, \dots h_N)$ is the output of the last hidden layer, and the cross-entropy [26] is used as the loss function.

$$Loss = -\sum_{i=1}^{N} L_i \log\left(p_i\right) \tag{10}$$

During the training stage, we use Adaptive Moment Estimation (Adam) [27] and the backpropagation algorithm to optimize the weight of the network until the training loss is less than or equal to a threshold.

3.4 Probability Weighted Localization Algorithm Based on Neural Network

After continuously sampling at a fixed location to obtain C feature images and inputting them into the trained network mentioned in 3.2, we can get C prediction results. There are N probability values $\left(p_1^c, p_2^c, \ldots, p_N^c\right)$ for the c-th prediction result, where represent the probability of the feature image at each RP. We use probability weighted method [28]–[30] to estimate location. The coordinate of each RP is multiplied by the corresponding probability weight, and the coordinate obtained after the summation can be taken as the estimated location of the c-th prediction result. We use average value as the estimated location for C feature images.

$$L_{test}^{Net} = \frac{1}{C}\sum_{c=1}^{C}\sum_{i=1}^{N} p_i^c \cdot l_i \tag{11}$$

3.5 CSI Correction Localization Algorithm

K-nearest neighbors, weighted K-nearest neighbor (WKNN), support vector machine (SVM), Bayesian estimator and neural networks, as popular algorithms, have been applied for localization based on fingerprinting, and the key to most of them is similarity function, which is used to measure the similarity between two sets of data. In statistics, correlation coefficients that reflect the direction and degree of trends between two variables are often used to analyze whether there is a correlation between two variables. Common similarity functions include Euclidean distance, Mahalanobis distance, Bhattacharyya distance [31], Pearson Product-moment correlation coefficient, Spearman's rank correlation coefficient and so on. If we can find an appropriate way to combine various localization algorithm that can complement each other, the accuracy and robustness of localization can be further improved.

The prediction results based on neural network can be roughly divided into two situations. Considering one prediction result, let $p_{\max}$ be the maximum probability out of N probabilities p_i. When the maximum probabilities $p_{\max}$ of prediction results are generally large, it can be considered that the network has a high credibility for the current output. The number of prediction results whose maximum probability value is not less than threshold ρ is C'. The proportion is defined as $R\left(p_{\max} \geq \rho\right)$, and ρ is not less than 0.5 normally. In this situation, the probability weighted localization algorithm mentioned in 3.4 is used to estimate location. When the maximum probabilities $p_{\max}$ of prediction results are generally small, it can be considered that the network has a low credibility for the current output. In this situation, other localization algorithm should be utilized to correct the position. We choose KNN in this paper.

$$L_{test} = \begin{cases} L_{test}^{Net} & R\left(p_{\max} \geq \rho\right) \geq \alpha \\ \dfrac{1}{k}\left(L_{test}^{Net} + \displaystyle\sum_{i=1}^{k-1} l_i^{sort}\right) & R\left(p_{\max} \geq \rho\right) < \alpha \end{cases} \tag{12}$$
$$R\left(p_{\max} \geq \rho\right) = \frac{C'}{C}$$

Calculate the similarity between the fingerprint in CSI_{test} of the test node and the interpolated fingerprint database after generalized extended interpolation CSI_{insert} to obtain the position l_i^{sort} of each RP in descending order of similarity.

Different similarity functions have different standards for measuring the similarity of CSI, and each has its own advantages and disadvantages. Euclidean distance usually has fine accuracy in localization based on fingerprinting. However, since the CSI amplitudes of 30 subcarriers at different times at a fixed location often have similar changing trends, or shapes, and their amplitudes may increase or decrease overall, the Euclidean distance does not fully extract and utilize CSI features that may cause large matching errors. Some researchers proposed to use Pearson correlation coefficient (PCC) as CSI fingerprint similarity function [10], [11]. PCC ranges from −1 to 1. Two variables are positively linearly related given PCC is 1, and negatively linearly related given PCC is −1. When the absolute value of PCC is 1 the variables are perfectly linearly related, and when PCC is 0 there is no linear correlation between the variables. Spearman's rank correlation coefficient is calculated based on the order of the data, so it may miss some information compared to PCC. Bhattacharyya distance performs well in histogram matching, which may enhance the CSI feature mentioned above perfectly. In this paper, we use Bhattacharyya distance to make similarity function defined as blow.

$$B\left(\overline{csi_m}, \overline{csi_q}\right) = 1 - \eta\left(\overline{csi_m}, \overline{csi_q}\right) = 1 - \sqrt{1 - \frac{\displaystyle\sum_{k=1}^{K}\sqrt{\left|\overline{H_k^m}\right| \cdot \left|\overline{H_k^q}\right|}}{\sqrt{\displaystyle\sum_{k=1}^{K}\left|\overline{H_k^m}\right| \cdot \sum_{k=1}^{K}\left|\overline{H_k^q}\right|}}} \tag{13}$$

where X, Y are two fingerprints to be checked, and $\eta(X,Y)$ stands for Bhattacharyya distance.

4. Analysis and Validation

In the experiment, we used Mi Router 4C as access point (AP) and ASUS laptop equipped with IWL 5300 NIC as mobile device. We installed the 64-bit version of 12.04 LTS Ubuntu Linux on the laptop, and CSI data receiving and reading was done through CSI Tool [32]. The data receiving process is that the mobile device first pings the AP at 100 Hz, and then the AP sends back a CSI data packet. There are 4 pairs of antenna pair and 30 subcarriers in each CSI data packet.

As shown in Fig. 5, there are 35 RPs that are 0.6 meters apart, which are red dots, and 15 test nodes that spread in

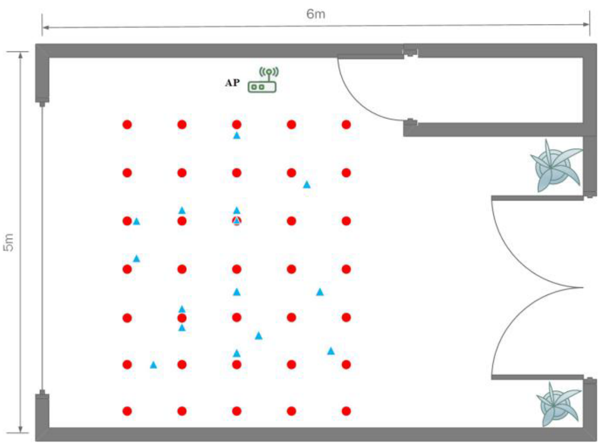

Fig. 5 Layout of the corridor for RPs and test nodes.

Table 1 Comparison of similarity functions.

Similarity Function	Mean Location Error(m)	Standard Deviation Location Error(m)	Maximum Location Error(m)
Euclidean distance	0.774	0.497	1.617
Pearson correlation coefficient	0.632	0.336	1.067
Spearman's rank correlation coefficient	0.615	0.348	1.067
Bhattacharyya distance	0.536	0.334	1.077

the environment randomly, which are blue triangles. In this 5 m × 6 m environment, the AP is placed closed to the wall. We collect 1000 CSI data packets at each RP in offline stage and 200 CSI data packets at each test node in online stage.

The anomalies of training data are eliminated by iForest. The parameters of iForest are described as follows: the number of training rounds is 1, the number of isolated trees is 85, the size of subsampling is 200, and the proportion of abnormal samples eliminated is 0.5%. And then we have CSI training data set with 35 RPs. In this paper, we propose CSI localization DenseNet in 3.2, and the network is trained in offline stage.

In online stage, we get the coordinate of test node roughly by probability weighted localization algorithm based on neural network, and the coordinates of $R\,(p_{\max} \geq 0.5) < 80\%$ test nodes are corrected by KNN based on Bhattacharyya distance.

4.1 Effect of Different Similarity Functions

Different similarity functions have different measurement standers. As shown in Table 1 and Fig. 6, Bhattacharyya distance has the smallest mean localization error and standard deviation localization error. Considering all kinds of errors, the Bhattacharyya distance is used as the similarity function of the correction localization algorithm.

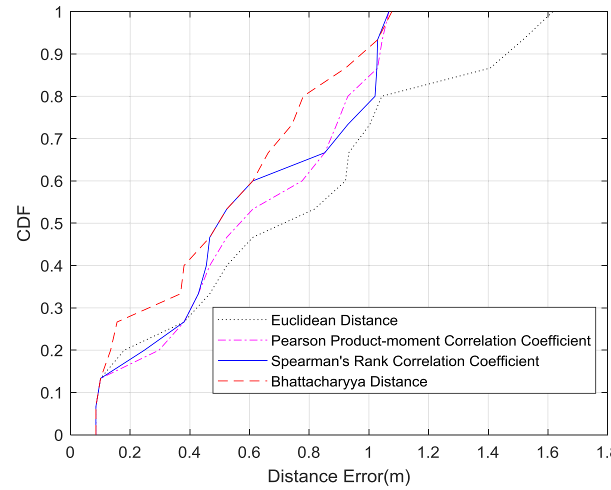

Fig. 6 CDF of localization errors for CorFi with different similarity functions.

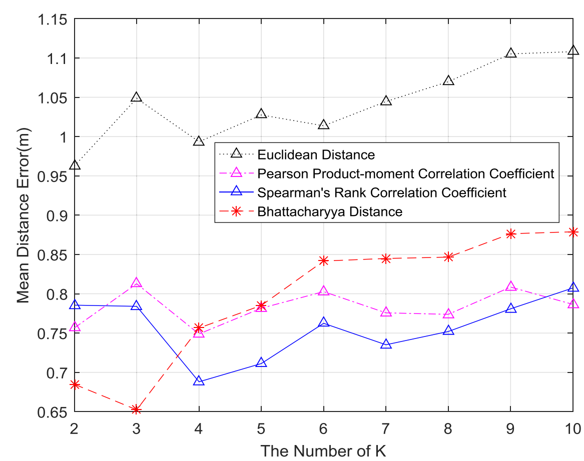

Fig. 7 Mean distance error of different parameter K.

4.2 Effect of Parameter K

The parameter K is the number of nearest neighbors in KNN algorithm. In CorFi, the prediction result of the network is also included in KNN, so the number of nearest neighbors needs to be exceed 1. When the parameter K is 1, CorFi degenerates into probability weighted localization algorithm based on neural network, which does not use other algorithm for location correction. When K is too high, the RPs far away from the test node are also introduced into location estimation, and usually these RPs without effective information diminish the localization performance, so we choose 3 as reasonable number of nearest neighbors in CorFi. (Fig. 7)

4.3 Effect of Interpolated Fingerprint

In the experiment, we use linear interpolation as a comparison. Fig. 8 shows that the interpolated fingerprint database achieves higher localization accuracy than original fingerprint database, and CorFi using generalized extended inter-

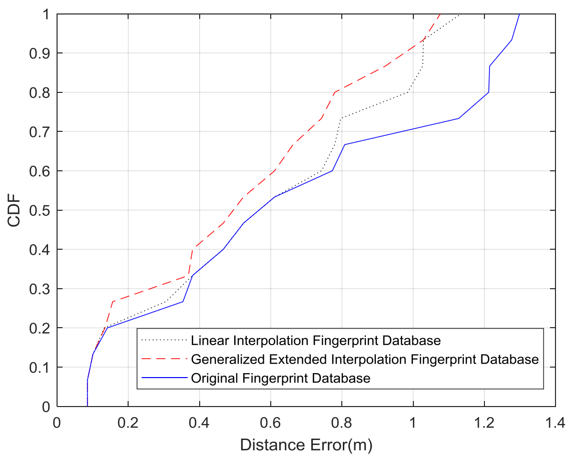

Fig. 8 CDF of localization errors for CorFi with different interpolations.

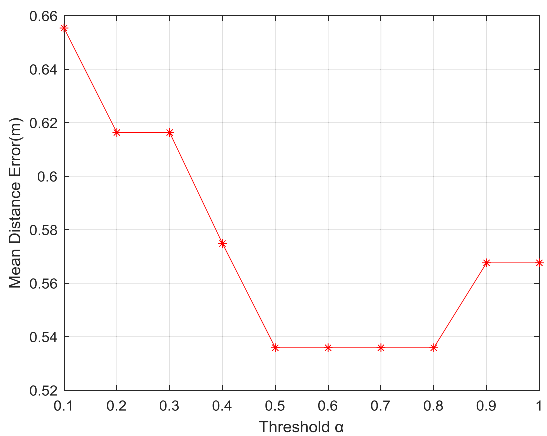

Fig. 9 Mean distance error of different proportion thresholds.

polation is better than linear interpolation.

4.4 Effect of Proportion Threshold α

CSI Correction Localization Algorithm mentioned in 3.5 selects localization method by judging whether the proportion of prediction results whose maximum probability value is greater than or equal to 0.5 is smaller than the proportion threshold α. Figure 9 shows that the mean localization error is large when α is too small or large. On the one hand, the prediction results with large localization error are not corrected when threshold α is too low. On the other hand, the prediction results with small localization error are 'corrected' when threshold α is too high, resulting in poor localization performance. According to Fig. 9, the proportion threshold α in this paper is 0.8.

4.5 Comparison with Existing Indoor Localization Algorithm

In this section, we compare probabilistic algorithm [33], kNN, DeepFi [12], ConFi [28] and CorFi. As shown in Fig. 10 and Table 2, ConFi has better localization performance than DeepFi, 80% of the localization errors of former is within 1.217 m, and 80% of the latter is within 1.342 m. CorFi further reduces the localization error, and effectively solves the problem of excessive localization error when the neural network localization performance is poor by correcting the position of prediction results with larger errors. 80% of the localization errors of CorFi is within 0.780 m.

Table 2 Comparison of different indoor localization algorithms.

Indoor localization algorithm	Mean Location Error(m)	Standard Deviation Location Error(m)	Maximum Location Error(m)
CorFi	0.536	0.334	1.077
ConFi	0.758	0.467	1.530
DeepFi	0.970	0.531	2.220
kNN	1.105	0.728	2.528
Probabilistic Algorithm	1.050	0.360	1.694

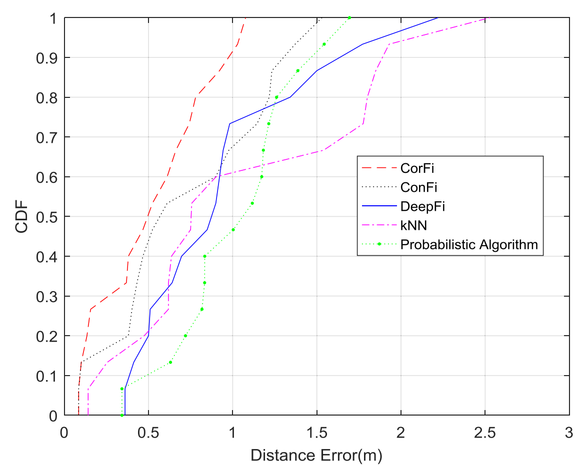

Fig. 10 CDF of localization errors for different indoor localization algorithms.

4.6 Comparison with Different Neural Networks

In this section, different neural networks are applied to compare the localization performance in proposed algorithm. We used LeNet5 [34] and VGG11 [35] to replace DenseNet, and we use the same training fingerprint database to train all neural networks. When the training loss is not greater than the threshold, the test fingerprint database is applied to verify each network. As shown in Table 3 and Fig. 11, CorFi reduces the mean location error by 29% compared with the probability weighted localization algorithm when Densenet is used, while it is 5% and 8% when LeNet5 and VGG11 are used, respectively.

5. Conclusions

In this paper, we presented a novel indoor localization algorithm named CorFi. We combined the neural network

Table 3 Comparison of different neural networks.

Method	Type of Neural Network	Mean Location Error(m)	Standard Deviation Location Error(m)	Maximum Location Error(m)
Probability Weighted Localization Algorithm Based on Neural Network	LeNet5	1.353	0.882	3.014
	VGG11	1.276	0.812	2.461
	DenseNet	0.758	0.467	1.530
CorFi	LeNet5	1.281	0.857	2.844
	VGG11	1.177	0.713	2.179
	DenseNet	0.536	0.334	1.077

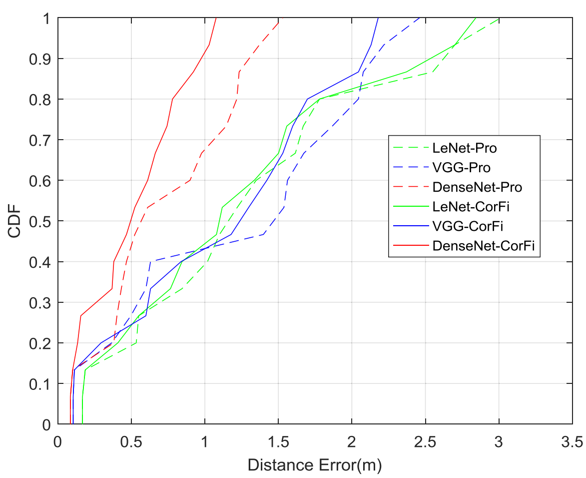

Fig. 11 CDF of localization errors for different neural networks.

fingerprinting with the KNN algorithm, which effectively remedy the shortcomings of probability weighted localization algorithm based on neural network, and improves the localization accuracy and robustness. The proposed feature image fully exploits the CSI information in time, frequency and space domain. The improved DenseNet was used to establish correspondence between CSI and spatial position, and the probability weighted localization algorithm was used to estimate location. We expanded the fingerprint database by generalized extended interpolation, which reduces manpower costs and provides a high-precision interpolation fingerprint database for correction localization algorithm during online stage.

Acknowledgments

This research was funded by Foundation of Zhejiang Province Education Department of China (Y202044275).

This research was funded by Policy-guided plans (international scientific and technological cooperation) “the Belt and Road” innovation cooperation project (BZ2019006).

References

[1] W. Kang and Y. Han, “SmartPDR: Smartphone-based pedestrian dead reckoning for indoor localization,” IEEE Sensors J., 2014, vol.15, no.5, pp.2906–2916, 2015.

[2] S. Pittet, V. Renaudin, B. Merminod, and M. Kasser, “UWB and MEMS based indoor navigation,” J. Navigation, vol.61, no.3, pp.369–384, 2008.

[3] Y.-S. Kuo, P. Pannuto, K.-J. Hsiao, and P. Dutta, “Luxapose: Indoor positioning with mobile phones and visible light,” Proc. 20th annual international conference on Mobile computing and networking, pp.447–458, 2014.

[4] K.P. Subbu, B. Gozick, and R. Dantu, “LocateMe: Magnetic-fields-based indoor localization using smartphones,” ACM Trans. Intell. Syst. Technol. (TIST), vol.4, no.4, pp.1–27, 2013.

[5] X. Li, J. Wang, and C. Liu, “A Bluetooth/PDR integration algorithm for an indoor positioning system,” Sensors, vol.15, no.10, pp.24862–24885, 2015.

[6] Q. Guo and W.C. Wong, “Tracking indoor pedestrian using Cricket indoor location system,” 2012 IEEE International Conference on Communication Systems (ICCS). IEEE, pp.453–457, 2012.

[7] S. Sen, B. Radunovic, R.R. Choudhury, and T. Minka, “You are facing the Mona Lisa: Spot localization using PHY layer information,” Proc. 10th international conference on Mobile systems, applications, and services, pp.183–196, 2012.

[8] S. Sen, R.R. Choudhury, B. Radunovic, and T. Minka, “Precise indoor localization using PHY layer information,” Proc. 10th ACM Workshop on Hot Topics in Networks, pp.1–6, 2011.

[9] K. Wu, J. Xiao, Y. Yi, M. Gao, and L.M. Ni, “FILA: Fine-grained indoor localization,” 2012 Proceedings IEEE INFOCOM, pp.2210–2218, 2012.

[10] J. Xiao, K. Wu, Y. Yi, and L.M. Ni, “FIFS: Fine-grained indoor fingerprinting system,” Proc. 2012 21st International Conference on Computer Communications and Networks (ICCCN), pp.1–7, 2012.

[11] Y. Chapre, A. Ignjatovic, A. Seneviratne, and S. Jha, “CSI-MIMO: Indoor Wi-Fi fingerprinting system,” Proc. 39th Annual IEEE Conference on Local Computer Networks, pp.202–209, 2014.

[12] X. Wang, L. Gao, S. Mao, and S. Pandey, “CSI-based fingerprinting for indoor localization: A deep learning approach,” IEEE Trans. Veh. Technol., vol.66, no.1, pp.763–776, 2016.

[13] X. Wang, L. Gao, and S. Mao, “CSI phase fingerprinting for indoor localization with a deep learning approach,” IEEE Internet Things J., vol.3, no.6, pp.1113–1123, 2016.

[14] Q. Song, S. Guo, X. Liu, and Y. Yang, “CSI amplitude fingerprinting-based NB-IoT indoor localization,” IEEE Internet Things J., vol.5, no.3, pp.1494–1504, 2018.

[15] Z.-H. Wu, Y. Han, Y. Chen, and K.J.R. Liu, “A time-reversal paradigm for indoor positioning system,” IEEE Trans. Veh. Technol., vol.64, no.4, pp.1331–1339, 2015.

[16] C.H. Hsieh, J.Y. Chen, B.H. Nien, “Deep learning-based indoor localization using received signal strength and channel state information,” IEEE Access, vol.7, pp.33256–33267, 2019.

[17] L. Zhao, H. Wang, P. Li, and J. Liu, “An improved WiFi indoor localization method combining channel state information and received signal strength,” 2017 36th Chinese Control Conference (CCC). IEEE, pp.8964–8969, 2017.

[18] Y. Xie, Z. Li, and M. Li, “Precise power delay profiling with commodity Wi-Fi,” IEEE Trans. Mobile Comput., vol.18, no.6, pp.1342–1355, 2019.

[19] Z. Yang, Z. Zhou, and Y. Liu, “From RSSI to CSI: Indoor localization via channel response,” ACM Comput. Surv. (CSUR), vol.46, no.2, pp.1–32, 2013.

[20] F.T. Liu, K.M. Ting, and Z.-H. Zhou, “Isolation forest,” Proc. 2008 eighth IEEE International Conference on Data Mining, pp.413–422, 2008.

[21] F.T. Liu, K.M. Ting, and Z.-H. Zhou, “Isolation-based anomaly detection,” ACM Trans. Knowl. Discov. Data, vol.6, no.1, pp.1–39, 2012.

[22] W. Shi, YI. Yan, and G. Xu, Generalized Extended Interpolation in Engineering Science, Science Press, Beijing, China, 2005.

[23] C. Liu, J. Shang, R. Li, and K. Yue, "Indoor dynamic environment localization algorithm based on transfer learning," Telecommunications Science, vol.34, pp.98–108, 2018.
[24] G. Huang, Z. Liu, L.V. Maaten, and K.Q. Weinberger, "Densely connected convolutional networks," Proc. IEEE Conference on Computer Vision and Pattern Recognition, pp.4700–4708, 2017.
[25] D.-A. Clevert, T. Unterthiner, S. Hochreiter, "Fast and accurate deep network learning by exponential linear units (ELUs)," arXiv preprint arXiv:1511.07289 2015.
[26] P.-T. De Boer, D.P. Kroese, S. Mannor, and R.Y. Rubinstein, "A tutorial on the cross-entropy method," Ann. Oper. Res., vol.134, pp.19–67, 2005.
[27] D.P. Kingma and J. Ba, "Adam: A method for stochastic optimization," arXiv preprint arXiv:1412.6980, 2014.
[28] H. Chen, Y. Zhang, W. Li, X. Tao, and P. Zhang, "ConFi: Convolutional neural networks based indoor Wi-Fi localization using channel state information," IEEE Access, vol.5, pp.18066–18074, 2017.
[29] K. Wu, J. Xiao, Y. Yi, D. Chen, X. Luo, and L.M. Ni, "CSI-based indoor localization," IEEE Trans. Parallel Distrib. Syst., vol.24, no.7, pp.1300–1309, 2013.
[30] X. Wang, X. Wang, and S. Mao, "ResLoc: Deep residual sharing learning for indoor localization with CSI tensors," 2017 IEEE 28th Annual International Symposium on Personal, Indoor, and Mobile Radio Communications (PIMRC), IEEE, pp.1–6, 2017.
[31] A. Bhattacharyya, "On a measure of divergence between two multinomial populations," Sankhyā: The Indian Journal of Statistics, vol.7, no.4, pp.401–406, 1946.
[32] D. Halperin, W. Hu, A. Sheth, and D. Wetherall, "Predictable 802.11 packet delivery from wireless channel measurements," ACM SIGCOMM Comput. Commun. Rev., vol.40, no.4, pp.159–170, 2010.
[33] T. Yu, A. Haniz, K. Sano, R. Iwata, R. Kosaka, Y. Kuki, G.K. Tran, J.-I. Takada, and K. Sakaguchi, "A guide of fingerprint based radio emitter localization using multiple sensors," IEICE Trans. Commun., vol.E101-B, no.10, pp.2104–2119, Oct. 2018.
[34] Y. LeCun, L. Bottou, Y. Bengio, and P. Haffner, "Gradient-based learning applied to document recognition," Proc. IEEE, vol.86, no.11, pp.2278–2324, 1998.
[35] K. Simonyan and A. Zisserman, "Very deep convolutional networks for large-scale image recognition," arXiv preprint arXiv:1409.1556, 2014.

Junna Shang graduated from the National Astronomical Observatories of the Chinese Academy of Sciences in 2006 with a Ph.D., and now works in college of Telcommunication Engineering, Hangzhou Dianzi University, engaged in teaching and scientific research.

Ziyang Yao studys for a master's degree in Electronics and Communication Engineering at the college of Telcommunication Engineering, Hangzhou Dianzi University.